Available online at www.sciencedirect.com
ScienceDirect
Bioelectrochemistry 72 (2008) 155–160
Bioelectrochemistry
www.elsevier.com/locate/bioelechem

Electrocatalysis of emodin at multi-wall nanotubes

Zhao-Hui Yin [1], Qiao Xu [1], Yi Tu, Qiu-Ju Zou, Jiu-Hong Yu, Yuan-Di Zhao *

Key Laboratory of Biomedical Photonics of Ministry of Education - Wuhan National Laboratory for Optoelectronics - Hubei Bioinformatics and Molecular Imaging Key Laboratory - Key Laboratory of Molecular Biophysics of the Ministry of Education, College of Life Science and Technology, Huazhong University of Science and Technology, Wuhan, Hubei, PR China, 430074

Received 5 September 2007; received in revised form 10 January 2008; accepted 11 January 2008
Available online 18 January 2008

Abstract

In this article, the electrochemical behavior of emodin at multi-wall carbon nanotube modified glassy carbon electrodes (MWNTs/GCE) was studied. The result showed that MWNTs/GCE had high electrocatalytic activity for emodin. And the electrocatalytic redox process was a two-charge-two-proton process. Diffusion coefficient (D_R) of 8.403×10^{-5} cm^2 s^{-1} of emodin was obtained. Further experiments demonstrated that the oxidative peaks increased linearly with emodin concentrations in the range of 1.0×10^{-6} to 1.0×10^{-4} M with a limit of detection of 3.0×10^{-7} M. This electrochemical method was accurate and reliable, therefore, it might provide a novel way for emodin detection.

Keywords: Carbon nanotube; Modified electrode; Emodin; Determination

1. Introduction

Carbon nanotube (CNT), discovered in 1991 [1], is one of the world wide hot spots due to its unique physical, chemical characters and its potential application foreground. Carbon nanotube may be regarded as a graphite sheet rolled up to form a tube and can be divided into single-wall carbon nanotube (SWNT) [2] and multi-wall carbon nanotube (MWNT) [3]. Carbon nanotube has unique structure, appropriate surface area, low resistance and high stability [4]. Because of its curved wall, electric charge transfer is quicker than that of the transfer in graphite, it can be used as an excellent electrode material [5]. Multi-wall carbon nanotube modified electrodes are easy to prepare, of low disturbance and high stability, they can be widely used in the detection of bioactive molecules, such as theophylline [6], hydrogen peroxide [7], guanine [8] and levodopa [9].

Emodin [1, 3, 8-trihydroxy-6-methylanthraquinone] (Fig. 1) is a biologically active natural compound extracted from the rhizomes of *Rheum palmatum* with anti-microbial, immunosuppressive and anti-inflammatory activities [10,11]. Emodin has strong anti-microbial activities because it can restrain the biosynthesis of the nucleic acid and respiration of bacteria, the mechanism of which lies in its effect of oxidation and dehydrogenation of sugar and the intermediate product of the sugar metabolism, oxidation and dehydrogenation of amino acid as well as restriction of protein synthesis. Recently, it was discovered that emodin can increase the repair of UV- and cisplatin-induced DNA damage in human cells, and elevate ERCC1 gene expression [12]. It was also found that emodin had the potential application foreground in the treatment of multiple organ dysfunction syndromes [13]. Therefore, the research and detection of emodin has important theoretical and practical significance.

Emodin can be chemically classified as an anthraquinone derivative with electro-activity. Current detections of emodin include spectroscopic method [14], oscillopolarography [15], micellar electrokinetic capillary chromatography [16], etc. Among these, the electrochemical methods have the advantage of celerity, simplicity and high sensitivity. For example, Zou etc. [15] studied the polarographic behavior and the mechanism of electrode reaction of emodin. It was found that there was a sensitive second derivative peak at −0.75 V (*vs.* SCE) when using single sweep oscillopolarography. This peak current

* Corresponding author. Tel.: +86 27 87792235; fax: +86 27 87792202.
E-mail address: zydi@mail.hust.edu.cn (Y.-D. Zhao).
[1] These authors contribute equally to this work.

1567-5394/$ - see front matter © 2008 Elsevier B.V. All rights reserved.
doi:10.1016/j.bioelechem.2008.01.005

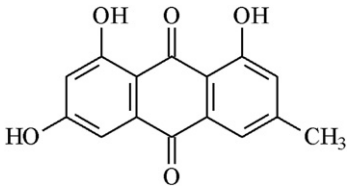

Fig. 1. Chemical structure of emodin.

increased linearly with emodin concentration in the range of 1.42×10^{-7} to 5.7×10^{-6} M and 7.1×10^{-6} to 7.1×10^{-5} M with a limit of detection (LOD) of 0.7×10^{-7} M.

In this paper, based on the advantage of quicker electric charge transfer of CNT, multi-wall carbon nanotube modified glassy carbon electrode was used to study the electrochemical behavior of emodin. It was discovered that multi-wall carbon nanotube modified glassy carbon electrode had better electrocatalytic effect for the redox of emodin than that of bare glassy carbon electrode. Electrochemical parameters were obtained and this electrochemical method was used to determine the unknown concentration of emodin sample solution extracted from *Rheum*. A controlled experiment showed that the result obtained from the electrochemical method was accurate and reliable. Thus, a novel possible way was provided for the detection of emodin.

2. Experimental

2.1. Instruments and reagents

The electrochemical experiments, cyclic voltammetric (CV) and chronocoulometric (CC) experiments were performed with an electrochemical workstation (CHI621A, CH Instruments, China) coupled with a conventional three-electrode cell. The working electrode was a multi-wall carbon nanotube modified glassy carbon electrode (MWNTs/GCE) or a bare glassy carbon electrode (GCE), the auxiliary electrode platinum wire, and the reference electrode saturated calomel electrode (SCE). All the potentials were given against the SCE. A pH meter (PHS-3C, Shanghai Precision Scientific Inc., China), ultrasonic cleaning device (DL-180A, Shanghai ZX equipment Ltd., China), transmission electron microscope (Tecnai G2 20, PEI, Netherlands) and UV–visible spectrophotometer (UV-2550, Shimadzu, Japan) were used. Pure emodin was obtained from Chinese Institute for the Control of Pharmaceutical and Biomedical Products (Beijing, China) with the purity of more than 98%. The rhizomes of rhubarb were purchased from the Hubei Chinese Herbal Medicine Resource Ltd. (Wuhan, Hubei, China) and identified as *Rheum officinal* Baill. MWNTs were prepared in the same way as reference [17]. Phosphate-buffered saline (PBS, pH 10.1, 0.1 M) and other reagents were of analytical grade. All solutions were prepared with twice-distilled water. The buffer solutions were purged with high-purity nitrogen for at least 10 minutes prior to experiments and a nitrogen environment was then kept over the solution in the cell. All experiments were performed at room temperature.

2.2. Preparation of the MWNTs/GCE

Crude MWNTs were ultrasonically agitated in 3 M HNO_3 for 1 h and refluxed in 5 M HCl for 4 h at 110 °C. After acid treatment, the samples were calcined in static air at 350 °C for about 2 h. 1 mg purified MWNTs were dispersed with the aid of ultrasonic agitation in 1 mL of N, N-dimethylformamide (DMF) to form 1 mg/mL black suspension. The bare GCE was polished with 0.05 μm alumina slurry, sonicated in acetone and twice-distilled water for 3 to 5 min, respectively. The cleaned GCE was then coated by 20 μL 1 mg/mL MWNTs black suspension. After dried in the air overnight to remove the solvent, the MWNTs/GCE was prepared.

2.3. Preparation of the emodin sample solution

Emodin was extracted from the rhizomes of rhubarb in the same way as reference [18]. This process was mainly as follows: a certain amount of the 80-mush-sized rhubarb rhizomes powder in 1:12 (w/v) chloroform–glycerol–sulfuric acid (20%) (4:1:1, v/v/v) was heated to reflux for 110 minutes. After cooling, the solution was filtered. The filtrate was washed three times with twice-distilled water. The organic phase was removed and distilled under vacuum to give solid power anthraquinone derivatives. Unknown concentration of emodin sample solution in PBS (pH 10.1, 0.1 M) was then prepared.

3. Results and discussion

3.1. TEM characterization of MWNTs

1 mg purified MWNTs were dispersed in 1 mL DMF to form 1 mg/mL black suspension. From the TEM image (Fig. 2), it can be clearly seen that MWNTs dispersed homogeneously and the MWNTs were about 10 nm in diameter.

3.2. Electrochemical behavior of emodin at MWNTs/GCE

After MWNTs/GCE was prepared, 1 mM $K_3Fe(CN)_6$ solution was used as probe to determine the microscopic areas of the bare GCE and MWNTs/GCE by CV. From CV graphs, it was found that $K_3Fe(CN)_6$ had a reversible redox peak at both bare GCE and MWNTs/GCE (figures were not displayed). For a reversible process, the anodic peak current is given by [19]:

$$I_{pa} = 2.69\times10^{5}\left(As/\left(\mathrm{mol\ V^{1/2}}\right)\right)n^{3/2}A\left(\mathrm{cm^2}\right)c_0\left(\mathrm{mol/cm^3}\right)\times\left[D_R\left(\mathrm{cm^2/s}\right)\right]^{1/2}[v(\mathrm{V/s})]^{1/2} \quad (1)$$

where I_{pa} refers to the anodic peak current, n is the electron transfer number, A is the surface area of the electrode, D_R is diffusion coefficient, c_0 is the concentration, v is the scan rate, in the parentheses are the units of the measurement ahead. As for $K_3Fe(CN)_6$, $n=1$, $D_R=5.90\times10^{-5}$ cm^2 s^{-1} [20]. From the slope of the $I_{pa}\sim v^{1/2}$ relation, the microscopic areas can be calculated, with 0.0345 cm^2 for the bare GCE, 0.0820 cm^2 for the MWNTs/GCE, indicating that the microscopic area of

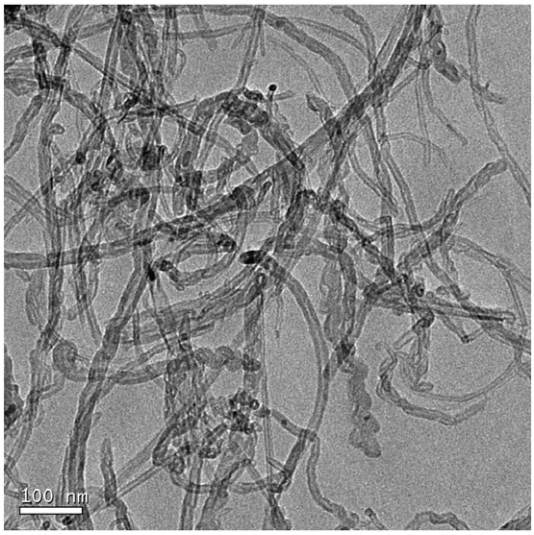

Fig. 2. TEM image of the purified MWNTs.

MWNTs/GCE increased significantly and was about 2.38 times larger than the microscopic area of bare GCE.

CV behaviors of emodin at bare GCE and MWNTs/GCE were studied respectively, the result is shown in Fig. 3. From Fig. 3, an irreversible peak can be seen at −0.332 V with the peak current of 7.50×10^{-7} A at bare GCE (Fig. 3, curve a), while the same irreversible peak shifted positively to −0.275 V at MWNTs/GCE with the peak current increased to 7.75×10^{-5} A (Fig. 3, curve b), about 103 times larger. It was also found that the peak currents of the irreversible oxidative peak increased linearly with the square root of scan rate in the range of 10 to 100 mV/s, indicating that it was a diffusion-controlled process. At the same time, a reductive peak can be seen at −0.777 V with the peak current of 7.50×10^{-6} A at bare GCE, while the same reductive peak shifted negatively to −0.853 V at MWNTs/GCE with the peak current increased to 9.878×10^{-5} A, about 13 times larger. These showed that the electrochemical response of emodin at bare GCE was very weak compared to the electrochemical response at MWNTs/GCE. The increased multiple of peak currents and microscopic areas were out of proportion, indicating that the increase of peak currents depended not only on the increase of microscopic area but mainly on the electrocatalytic effect of MWNTs. Moreover, another oxidative peak was observed at −0.728 V at MWNTs/GCE while there was only an inconspicuous oxidative process observed at GCE with much smaller peak current. The result of all these demonstrated that MWNTs/GCE has significant electrocatalytic effect for emodin, thus can be used for the detection of emodin.

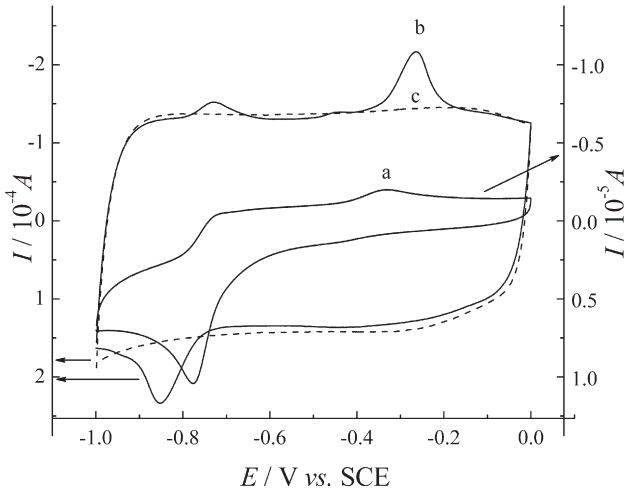

Fig. 3. CV curves of bare GCE (a) and MWNTs/GCE (b) in 1.0×10^{-5} M emodin solution (PBS, pH 10.1) and MWNTs/GCE (c) in PBS at a scan rate of 100 mV/s.

3.3. Electrochemical behavior of emodin at different pH values

The redox process of anthraquinone derivatives was frequently related to proton participation; therefore the electrochemical behavior of emodin at different pH values was studied. The relationship between the peak currents of the irreversible peak of the emodin at MWNTs/GCE and pH values were shown in Fig. 4. It can be seen that the peak potentials of the irreversible peaks shifted negatively as pH increased (Fig. 4A), indicating that this electrochemical process involving proton

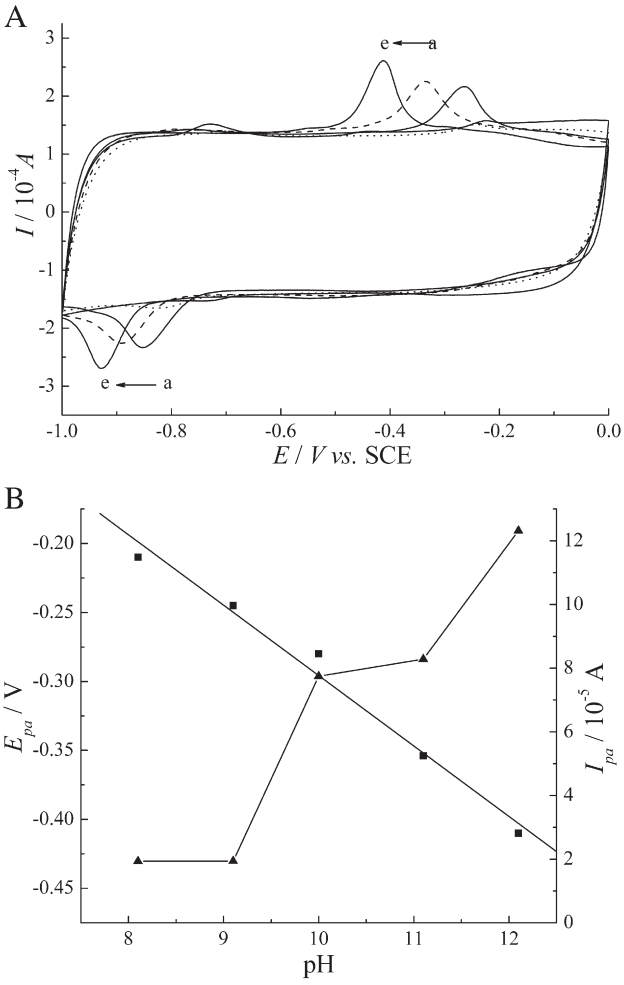

Fig. 4. (A) CV curves of MWNTs/GCE in 1.0×10^{-5} M emodin solution at a scan rate of 100 mV/s, pH from a to e: 8.1, 9.1, 10.1, 11.1, 12.1. (B) Relationship between E_{pa}, I_{pa} and pH values.

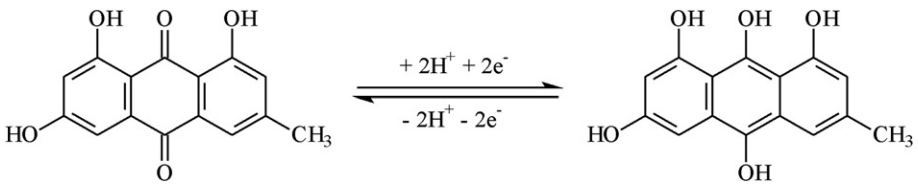

Fig. 5. Redox mechanism of emodin at MWNTs/GCE.

participation [21]. The peak potential of the irreversible peak and pH fitted linearly according to the following equation: $E_{pa}/V = 0.215 - 0.053\text{pH}$ ($R = 0.991$) (Fig. 4B), the slope of the E_{pa} and pH was near to the theoretic value of −0.056 V/pH when the number of participated protons and electrons was equal [22,23].

In the later experiments, emodin would be extracted from the rhizomes of *Rheum* which contained various types of anthraquinone derivatives, and the best pH was 10.1 in order that more emodin could be extracted with less impurity such as aloe-emodin [18], so the pH of 10.1 is selected.

3.4. The parameters of the electrochemical processes of emodin

3.4.1. Determination of electron transfer number

Relationship between peak current of the irreversible oxidative peak and scan rate was studied, the peak current increased as the increase of scan rate, and following equation was obtained: E_{pa} (V) = −0.218 + 0.0625 lg(v (V/s)), $R = 0.999$. According to Laviron's theory [24], for an irreversible process the following equation exists:

$$E_{pa}(\text{V}) = E^{0'}(\text{V}) + 2.303RT/[\alpha nF](\text{V}) + \lg[RT/[\alpha nF](\text{V})k^0(\text{cm/s})v(\text{V/s})] \quad (2)$$

where α refers to electronic transmission coefficient and is usually 0.5 [25], k^0 is the standard rate constant, n is the electron transfer number, v is the scan rate, $E^{0\prime}$ is the formal potential, in the parentheses are the units of the measurement ahead. n can be calculated to be 2, and because the number of participated protons and electrons was equal, it was a two-charge-two-proton process. Therefore, the proposed redox mechanism for emodin at MWNTs/GCE can be written as follows (Fig. 5) [15]:

3.4.2. Determination of the diffusion coefficient

The diffusion coefficient of emodin was determined at the MWNTs/GCE using CC (Fig. 6). For a diffusion-controlled

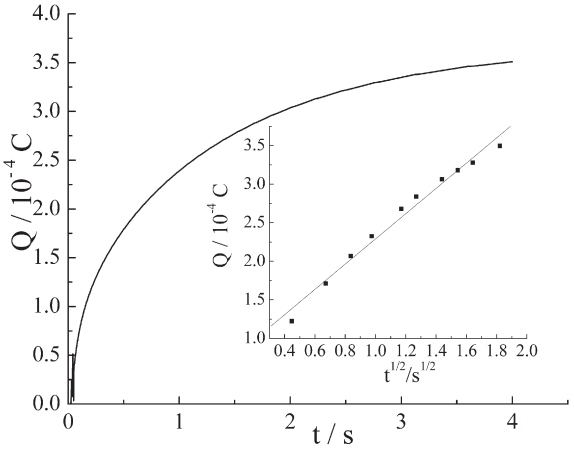

Fig. 6. Plot of Q against t for the MWNTs/GCE in 1.0×10^{-5} M emodin PBS solution. Insert: plot of Q against $t^{1/2}$.

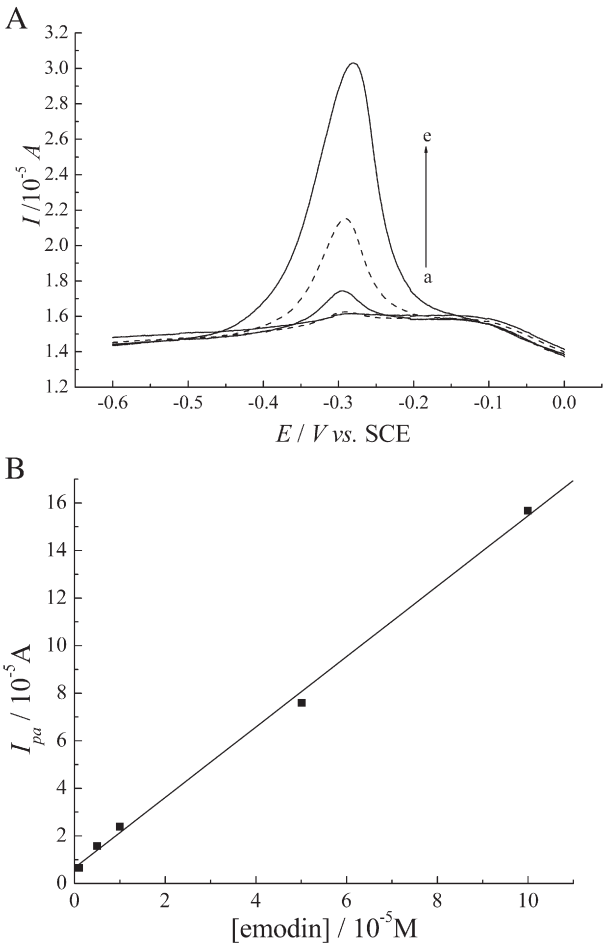

Fig. 7. (A) The irreversible oxidative peak of different concentration emodin at MWNTs/GCE. from a to e: 1.0×10^{-6}, 5.0×10^{-6}, 1.0×10^{-5}, 5.0×10^{-5}, 1.0×10^{-4} M. (B) The peak currents of the irreversible oxidative peak as the function of concentrations.

electrochemical process, the following Cottrell equation [26] exists:

$$Q = \frac{2n[F(\mathrm{C/mol})]A(\mathrm{cm^2})[D_R(\mathrm{cm^2/s})]^{1/2}c_0\left(\mathrm{mol/cm^3}\right)[t(\mathrm{s})]^{1/2}}{\pi^{1/2}} + Q_{dl}(\mathrm{C}) \quad (3)$$

where n refers to electron transfer number, F is Faraday constant 96,500 C/mol, A is the surface area of an electrode, D_R is diffusion coefficient, c_0 is the concentration. The potential step was from 0.1 to 0.5 V (Fig. 6). Based on the slope of $Q \sim t^{1/2}$ curve, 1. 637×10^{-4} C $s^{-1/2}$ (R=0.992), in the parentheses are the units of the measurement ahead, the diffusion coefficient (D_R) of emodin was estimated as 8.403×10^{-5} cm^2 s^{-1}.

3.5. The application of CV for the detection of emodin

Based on the experiments mentioned above, MWNTs/GCE was used to study emodin solutions of different concentrations (Fig. 7A). The result showed that the peak current of the irreversible oxidative peak increased linearly with the concentration of emodin in the range of 1.0×10^{-6} to 1.0×10^{-4} M (Fig. 7B). The linear regression equation was expressed as $I_{pa}/\ 10^{-5}$ A= $0.659 + 1.481c\ /\ 10^{-5}$ M, R=0.999 (n=5), with a limit of detection (LOD) of 3.0×10^{-7} M. Further experiments showed that MWNTs/GCE was of good reproducibility and reliability.

As an anthraquinone derivative, emodin has strong absorbance in the wavelength range of visible light [14]. Fig. 8 is the UV–visible spectra of pure emodin with different concentrations. In order to verify the effectiveness of this electrochemical method for the detection of emodin, the unknown concentration of emodin sample solution extracted from the rhizomes of *Rheum officinal* Baill was determined by electrochemical method and UV–visible spectrometry respectively. The UV–visible spectrometry result showed that the concentration of emodin is 4.90×10^{-5} M, while 4.81×10^{-5} M for CV result using MWNTs/GCE, which was close to the former one. This result confirmed that the electrochemical method for the detection of emodin was accurate and reliable.

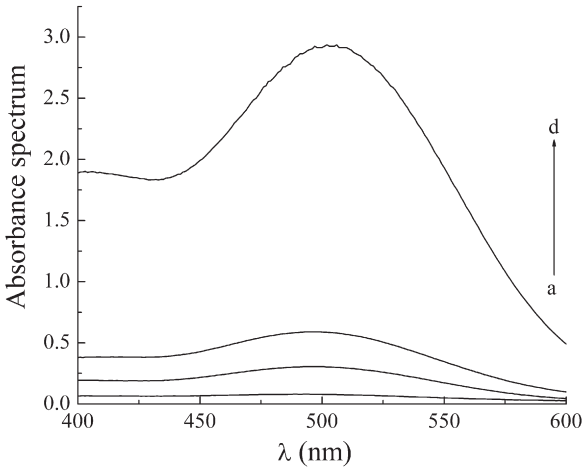

Fig. 8. UV–visible spectra of emodin with different concentration, from a to d: 1.0×10^{-5}, 5.0×10^{-5}, 1.0×10^{-4}, 5.0×10^{-4} M.

4. Conclusion

In this paper, the electrochemical behavior of emodin at MWNTs/GCE was studied. It was found that emodin presented better electrochemistry behavior at MWNTs/GCE, and the peak currents of the irreversible oxidative peak increased linearly with the concentration of emodin. The result of the detection of emodin by this electrochemical method matched that obtained by UV–visible spectrometry. Therefore the determination emodin at MWNTs/GCE was accurate and reliable, and thus a novel possible way for the detection of it is provided.

Acknowledgements

The work was supported by the National Natural Science Foundation of China (Grant No. 30670553, 30370387), the Program for Distinguish Young Scientist of Hubei Province (2006ABB020). We also thank Analytical and Testing Center (Huazhong University of Science & Technology) for the help in TEM measurement.

References

[1] S. Iijima, Helical microtubules of graphitic carbon, Nature 354 (1991) 56–58.
[2] S. Iijima, T. Ichihashi, Single shell carbon nanotubes of 1-nm diameter, Nature 363 (1993) 603–605.
[3] J.X. Wang, M.X. Li, Z.J. Shi, N.Q. Li, Z.N. Gu, Electrocatalytic oxidation of 3, 4-dihydroxyphenylacetic acid at a glassy carbon electrode modified with single-wall carbon nanotubes, Electrochim. Acta 47 (2001) 651–657.
[4] J.B. He, C.L. Chen, J.H. Liu, Study of multi-wall carbon nanotubes self-assembled electrode and its application to the determination of carbon monoxide, Sens. Actuators, B 99 (2004) 1–51.
[5] B. Zhang, J. Liang, C.L. Xu, B.Q. Wei, D.B. Ruan, D.H. Wu, Electric double-layer capacitors using carbon nanotube electrodes and organic electrolyte, Mater. Lett. 51 (2001) 539–542.
[6] Y. Zhu, Z. Zhang, D. Pang, Electrochemical oxidation of theophylline at multi-wall carbon nanotube modified glassy carbon electrodes, J. Electroanal. Chem. 581 (2005) 303–309.
[7] J. Wang, M. Musameh, Y. Lin, Solubilization of carbon nanotubes by nafion toward the preparation of amperometric biosensors, J. Am. Chem. Soc. 125 (2003) 2408–2409.
[8] Z. Wang, S. Xiao, Y. Chen, β-Cyclodextrin incorporated carbon nanotubes-modified electrodes for simultaneous determination of adenine and guanine, J. Electroanal. Chem. 589 (2006) 237–242.
[9] X. Yan, D. Pang, Z. Lu, J. Lu, H. Tong, Electrochemical behavior of L-dopa at single-wall carbon nanotube-modified glassy carbon electrodes, J. Electroanal. Chem. 569 (2004) 47–52.
[10] T.H. Tsai, Analytical approaches for traditional Chinese medicines exhibiting antineoplastic activity, J. Chromatogr. B: Anal. Technol. Biomed. Life Sci. 764 (2001) 27–48.
[11] F. Yang, T. Zhang, G. Tian, H. Cao, Q. Liu, Y. Ito, Preparative isolation and purification of hydroxyanthraquinones from *Rheum* officinale Baill by high-speed counter-current chromatography using pH-modulated stepwise elution, J. Chromatogr., A 858 (1999) 103–107.
[12] L.C. Chang, H.M. Sheu, Y.S. Huang, T.R. Tsai, K.W. Kuo, A novel function of emodin: enhancement of the nucleotide excision repair of UV- and cisplatin-induced DNA damage in human cells, Biochem. Pharmacol. 58 (1999) 49–57.
[13] Z.Y. Chen, Q.H. Qi, L.X. Liu, M.A. Tao, J. Xu, L. Zhang, L.N. Yan, Effects of emodin on Ca^{2+} signal transduction of smooth muscle cells in multiple organ dysfunction syndrome, J. Surg. Res. 131 (2006) 80–85.
[14] X.M Sun, C. Ma, S.J. Wu, X.Y. Wang, D.M. Cha, Spectrophotometric determination of *Rheum* emodin and its application, J. South-Cent. Univ. Natl. (Nat. Sci.) 20 (2001) 13–16.

[15] H. Zou, Z.B. Yuan, Investigation on electrochemical behavior of emodin and its application, Acta Pharm. Sinica 32 (1997) 310–313.
[16] Y.Y. Zong, M.T. Yu, Z.Q. Zhu, C.T. Che, Micellar electrokinetic capillary chromatography separation and determination of Chinese traditional medicine-several rheum species, Acta Pharm. Sinica 30 (1995) 594–598.
[17] Y.D. Zhao, W.D. Zhang, H. Chen, Q.M. Luo, S.F.Y. Li, Direct electrochemistry of horseradish peroxidase at carbon nanotube powder microelectrode, Sens. Actuators, B 87 (2002) 168–172.
[18] Q.H. Chen, H.S. Dai, X.L. Su, Studies on Chinese rhubarb XXX I. Improved method for systematic isolation of anthraquinone derivatives from rhubarb, Nat. Pro. Res. Dev. 13 (2001) 58–60.
[19] L.R. Faulkner, Electrochemical Method, Fundamental and Applications, (2nd edition), Wiley, New York, 2001.
[20] S.F. Wang, Q. Xu, Electrochemical parameters of ethamsylate at multi-walled carbon nanotube modified glassy carbon electrodes, Bioelectrochemistry 71 (2006) 1–5.
[21] R.N. Iyer, W.E. Schmidt, Observations on the direct electrochemistry of bovine copper–zinc superoxide dismutase, Bioelectrochem. Bioeng. 27 (1992) 393–404.
[22] A.M. bond, Modern Polarographic Methods In Analytical Chemistry, Marcel Dekker, New York, 1980, p. 29.
[23] L. Meites, Polarographic Techniques, 2nd edition, Wiley, New York, 1965, p. 282.
[24] E. Laviron, L. Roullier, Electrochemical reaction with adsorption of the reactants and electrosorption. Simple analytical solutions for a Henry isotherm, J. Electroanal. Chem. 443 (1998) 195–207.
[25] E. Laviron, Adsorption autoinhibition and autocatalysis in polarography and linear potential sweep voltammetry, J. Electroanal. Chem. 52 (1974) 355–373.
[26] A.J. Bard, L.R. Faulkner, Electrochemical Methods-Fundamentals and Applications, John Willey & Sons, Inc., 1980, p. 166.